Associations of Alkyl Carbonates: Intermolecular CH⊙⊙⊙ O Interactions

ARTICLE *in* THE JOURNAL OF PHYSICAL CHEMISTRY A · NOVEMBER 2001

Impact Factor: 2.69 · DOI: 10.1021/jp0126614

2 AUTHORS:

Yixuan Wang
Albany State University
55 PUBLICATIONS **1,413** CITATIONS
SEE PROFILE

Perla B. Balbuena
Texas A&M University
245 PUBLICATIONS **5,755** CITATIONS
SEE PROFILE

Associations of Alkyl Carbonates: Intermolecular C−H···O Interactions

Yixuan Wang* and Perla B. Balbuena*

Department of Chemical Engineering, University of South Carolina, Columbia, South Carolina 29208

Received: July 11, 2001; In Final Form: August 23, 2001

Self- and cross-associations of cyclic as well as linear carbonates such as ethylene carbonate (EC), propylene carbonate (PC), vinylene carbonate (VC), and dimethyl carbonate (DMC) are investigated with ab initio (MP2) and density functional theory (DFT) methods. The results show that cyclic and linear carbonates associate mainly through the intermolecular interactions of C−H···O. The basis set superposition error and zero-point energy-corrected binding energy, D_0(BSSE), for the global minimum of the linear carbonate DMC dimer (1.7 kcal/mol at B3LYP/6-311++G**) is much lower than those of the cyclic carbonates, and for the involved cyclic carbonates, it decreases in the following order: 5.1 (EC) ≈ 5.1 (EC/PC) > 4.7 (PC) > 3.9 (PC/VC) ≈ 3.8 (EC/VC) > 3.0 (VC). The dimer of DMC with EC (D_0(BSSE) = 2.8 kcal/mol) is also much less stable than the EC and PC dimers. Consistent with experimental findings, the results indicate that PC may also associate with EC molecules in their mixture; therefore, the cyclic carbonate molecules apparently still behave like associates instead of free molecules. However, EC molecules would be more free in a DMC/EC mixture because of weak intermolecular interactions. On the basis of the atoms-in-molecules (AIM) calculations, the C−H···O interactions may be classified as hydrogen bonds, although the C−H···O interaction exhibits a bond contraction and a blue vibrational frequency shift as compared with the monomer when the proton donor is linked with saturated molecules such as EC/PC/DMC, whereas it shows a C−H stretch and a red shift for the case of a proton linking with an unsaturated carbon such as VC. Such a difference perhaps arises from the opposite effect of a C−H bond stretch upon the monomer dipole moment. In line with the AIM analysis, the electron localization function technique (ELF) nicely demonstrates the existence of clear C−H···O interactions for VC dimers and trimers, which demonstrates the ability of the ELF procedure to characterize C−H···O systems.

Introduction

Cyclic alkyl carbonates, such as ethylene carbonate (EC), propylene carbonate (PC), and their linear analogue, dimethyl carbonate (DMC), and their mixtures are widely used as solvents of electrolytes in lithium-ion batteries.[1] EC has been proposed as a better solvent than PC because of its higher dielectric constant (89.8 vs 66.7 at 40 °C) and lower viscosity, which favors salt dissociation and enhances ionic diffusion rates. However, EC is a solid at room temperature (melting point of 36.2 °C). Therefore, mixtures of EC with liquid solvents such as PC and linear carbonates are required for practical applications. The performance of such mixtures depends to some extent on the interactions of carbonate molecules, i.e., their self- and cross-associations. The high dielectric constant of EC suggests a considerably organized network of polar molecules like H_2O. FTIR and Raman spectroscopic studies of Klassen et al.[2] indicated that strong self-association indeed exists among EC molecules. Very recently, classic molecular dynamics (MD) simulations and quantum mechanical (QM) calculations of EC have also been done to investigate its association properties.[3] Radial distribution functions (rdf) from the carbonyl oxygen to the hydrogen atom gave further evidence about EC's self-association; however, QM calculations did not yield stable complexes.[3] Additionally, Klassen's results also suggested that strong self-associations of EC remain unaltered in the presence of PC molecules, but they are disrupted by DMC and other linear carbonates. This suggests that DMC would be a better cosolvent than PC for EC because destruction of its network structure increases the fluidity of EC-based solutions. Recently, vinylene carbonate (VC) and other unsaturated carbonates have begun to be used as EC/PC-based solvent additives to modify the formation of a passivation solid electrolyte interfacial film (SEI), which results upon the solvent/cosolvent/additive reduction.[4] The self- and cross-association of the additive with the carbonate solvents could also affect its specific role; hence, a deeper understanding of its association properties is necessary to understand its behavior.

Carbonates probably associate mainly by the C−H···O intermolecular interactions between the carbonyl oxygen of one molecule as proton acceptor and the C−H group of another molecule as proton donor. Such interactions have been a quite active topic in the recent years because of its widespread occurrence from the gas phase[5] to liquid phase with biological interest[6−8] and even to crystalline environments.[9] On the other hand, it is well-known that the X−H bond will be stretched with a red shift of its vibrational frequency upon usual X−H···Y H-bond (e.g., O−H···O, F−H···F, etc.) formation; however, in some cases, C−H···O behaves oppositely, i.e., the C−H bond contraction accompanied by a blue shift of its vibrational frequency,[10−12] hereby it is called an anti-hydrogen bond. Because of the lower electronegativity of the carbon atom, there is an agreement that the C−H···O interactions represent specific interactions due to more than simple electrostatic forces between the partial negative charge on the oxygen and a positive charge that accumulates on C−H, despite the fact that they are weaker

* To whom correspondence should be addressed. E-mail for Y.W.: wangyi@engr.sc.edu. E-mail for P.B.B.: balbuena@engr.sc.edu.

10.1021/jp0126614 CCC: $20.00
Published on Web 10/04/2001

than conventional (e.g., O−H···O) H-bond interactions in some cases.[11,13,14] On the other hand, some controversies have emerged as to whether the C−H···O interaction is fundamentally different from the conventional H-bond and about the origin of its unusual behavior.[11] In a recent paper extensively examining the C−H···O interactions between $F_nH_{3-n}CH$ as proton donors and several acceptors, such as H_2O, CH_3OH, and H_2CO, as well as the water dimer, Gu et al.[11] showed that fundamental distinctions do not exist between the C−H···O and O−H···O interactions, although the O−H bond has been shown to stretch and undergo a red shift in its vibrational frequency upon formation of a H-bond, whereas the behavior of C−H followed the opposite trend. The inspection of a set of topological criteria based on atoms-in-molecules (AIM)[15] and used to characterize conventional H-bonds shows no essential difference between the two sorts of CH···π interactions with normal (C−H bond stretch) as well as antinormal (C−H bond contraction) properties for the proton donors, C−H, of H-bond.[16] Consistent with the behavior of C−H···O interactions,[11] C−H donors with an sp^3 hybridization carbon show a bond contraction accompanied by a blue shift of its vibrational frequency; however, a stretch and a red shift are observed for the donor of hydrogen linked with an unsaturated carbon (sp hybridization) such as CHCH and HCN. Muchall[17] found that the intramolecular C−H···O interaction in aromatic *N*-sulfinylaniline, i.e., phenyl−N═S═O, also fulfills the criteria of a H-bond and results in contraction of the C−H bond (1.083 vs 1.086 Å) and a blue shift of 26 cm^{-1} of the C−H-stretching frequency. In the present article, we use density functional theory (DFT)/ab initio method taking VC and EC as examples of C−H donors with sp^2 and sp^3 hybridization to investigate the C−H···O interactions in their complexes and to identify such weak interactions with two state-of-the-art techniques, electron localization function (ELF)[18,19] and AIM.[15]

Although DFT can bring about very reliable results for strongly bonded ionic, covalent, and most conventional H-bond systems,[20] significant problems can be encountered for van der Waals and weak H-bond systems.[21,22] Recent studies have found that the failure of some density functionals in describing van der Waals and other weak interactions can be attributed to the behavior of the exchange functional in the region of low density and large density gradient[23] and that indeed several generalized gradient approximations (GGA) can provide a good description for weak bonding.[23−26] To get reasonable pictures of the complexes through weak C−H···O interactions in carbonates, the present study applies the current DFTs to VC and EC systems as well.

Computational Details

To select a proper DFT for the C−H···O complex systems, some of the most frequently used functionals have been employed for VC dimer. The exchange functionals are Becke's GGA functional (B),[27] GGA exchange functional of Perdew-Wang 1991 (PW91),[28] and Becke's three-parameters hybrid GGA/exact-exchange functional (B3).[29] The correlation functionals are Lee−Yang−Parr GGA functional (LYP)[30] and Perdew-Wang 1991 correlation functional (PW91).[28] Six different DFT functionals result from combinations of these exchange and correlation functionals: BLYP, BPW91, B3LYP, B3PW91, PW91LYP, and PW91PW91. Geometries were fully optimized with the basis set 6-311++G(d,p). The same level was used to calculate the corresponding harmonic vibrational frequencies, which enable us to confirm the minima and to evaluate the corresponding zero-point energy (ZPE) corrections. For comparison, conventional ab initio HF and MP2 calculations were carried out.

The binding energies are defined as

$$\Delta E = nE(\text{monomer}) - E(n\text{-mer}), \quad n = 2, 3 \qquad (1)$$

With the use of the continuous basis set superposition error (BSSE) and ZPE and with calculation of thermal corrections (T = 298.2 K), the results are termed as D_e(BSSE), D_0(BSSE), and D_T, respectively. The BSSE corrections were estimated using the counterpoise method of Boys and Bernardi.[31] The results show that the ZPE may account for as much as 25% of the total interaction energy, and thermal corrections approach to 50% in VC containing complexes. In this respect, it is worth noting that care should be taken, when compared with literature results, to ensure consistency.

Another interesting phenomenon associated with *n*-mers ($n \geq 3$) of a normal H-bond system is its cooperativity effect, i.e., the enhancement of the first H-bond between a donor and an acceptor once a second H-bond is formed between the third molecule and one of the first two molecules. The indication of this effect is a bigger bond stretch and an enhanced frequency shift of the proton donor. The cooperative factor, A_b, was defined as the ratio of the shift of the donor stretching frequency in the trimer ($\Delta\nu'$) to that in the dimer ($\Delta\nu$),[32]

$$A_b = \Delta\nu'/\Delta\nu \qquad (2)$$

To analyze chemical bondings, ELF[18,19] as well as AIM[15] techniques were employed to visualize the interactions within complexes. ELF was developed as a measure of the probability of finding an electron in the neighborhood of another electron with the same spin. By definition, it ranges between 0 and 1. The higher the ELF value, the smaller is the probability of finding a second parallel-spin electron near the reference point. Hence, a large value of ELF means that the reference electron is highly localized. High ELF values locate the regions that can be interpreted as covalent bonds, lone pairs, and inert cores, while low values are typical for the regions between electronic shells and the regions where van der Waals and other weak types of interactions dominate. Extensive applications of ELF to various molecules, atomic clusters, molecular clusters, and H-bond interactions, especially relevant to the present study, and even to solid systems[33−37] indicate that this technique yields meaningful, easily understandable, and visually directive patterns of the interactions between vicinal atoms.

DFT, ab initio, and AIM calculations were performed with the Gaussian 98 (revision A9) program package,[38] and two-dimensional (2D) evaluations of ELF were done by the separated programs,[39] which are interfaced to MOLPRO.[40]

Results and Discussions

A. Geometric and Energetic Properties. *VC Dimer*. The ground state of VC possesses planar geometry with C_{2v} symmetry. Three dimer minima have been obtained by pointing the C−H bond toward the carbonyl oxygen, as shown in Chart 1. They are a planar structure, **D1** (C_s), a bifurcated structure, **D2**, with higher symmetry (C_{2v}), and a T-shaped structure, **D3** (C_s), of two monomer planes perpendicular to each other. The calculated energetic data and binding characteristics of **D1**, **D2**, and **D3** from a series of methods are collected in Table 1. In the case of **D1**, BSSE corrections (the differences between the third and forth columns) of BLYP, BPW91, B3LYP, and B3PW91 are very comparable (0.24, 0.28, 0.26, and 0.28 kcal/mol, respectively), while those from the PW91 exchange functional with each of the correlation functionals, LYP and PW91, are comparatively higher (0.41 and 0.44 kcal/mol for

CHART 1: Optimized Geometries (B3LYP/6-311++G(d,p)) of Carbonate Monomers and Their Dimers. A Black Ball Stands for an Oxygen Atom, a Big White One for a Carbon Atom, and a Small One for a Hydrogen Atom

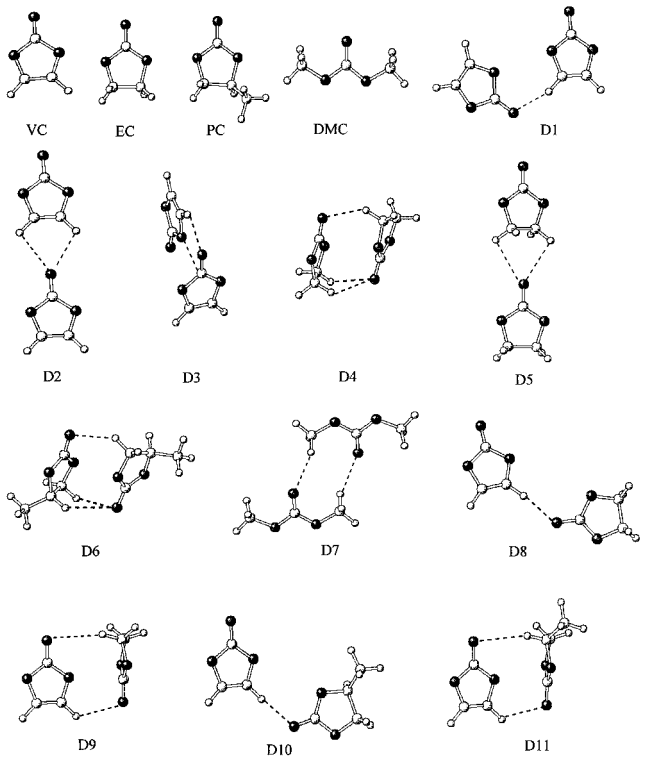

PW91LYP and PW91PW91, respectively). It is noted that BSSE corrections are much higher at the MP2 level, approaching 2.05, 1.88, 1.81, and 1.79 kcal/mol with 6-31G*, 6-31+G**, 6-311G**, and 6-311++G** basis sets, respectively. ZPE corrections from density functional methods (the differences between the forth and fifth columns) range from 0.37 kcal/mol (BPW91) to 0.48 kcal/mol (PW91PW91). In line with the findings of MÓ et al.,[41] the thermal corrections (differences between the fifth and sixth column) at 298.2 K associated with translational, rotational, and vibrational degrees of freedom are not negligible either. For example, they account for as much as about 1.4 kcal/mol for the VC dimer at the PW91LYP/6-311++G(d,p) level.

Regarding the binding energies, generally the Becke GGA exchange functional (B) with correlation functional of either LYP or PW91 results in the lowest values, especially before thermal correction. The hybrid exchange functional, B3, results are higher than those from B by approximately 25% for ΔE, D_e(BSSE), and D_0(BSSE); however, the thermal-corrected D_T values are nearly the same as those from B. The binding energies are further considerably enhanced with the exchange functional PW91. With respect to geometric properties, the bond distance between the donor hydrogen and the carbonyl oxygen (R) is only a little shortened by about 0.05 Å, and the angles of C−H···O (A) even agree within 0.1°. Although the distances R again remain rather close to those predicted from both B and B3, the angle A deviates further from linear geometry, e.g., 161.0° and 165.5° at the PW91LYP and PW91PW91 levels, respectively. At the given exchange functionals, the correlation functional LYP systematically brings about 0.5 kcal/mol higher binding energies than the correlation functional PW91. The present trends obtained from different exchange and correlation functionals qualitatively agree with their performance in van der Waals molecules and N−H···π weak H-bond systems.[23,26]

TABLE 1: Energy Differences Including Relevant Corrections, ΔE, D_e(BSSE), D_0(BSSE), and D_T (kcal/mol), the Distances between H and Carbonyl O, R (Å), and the Angles of C−H···O, A (deg), for Vinylene Carbonate (VC) Dimers, D1, D2, and D3, and Water Dimer, WD, Calculated with the Several Listed Methods, but the Same Basis Set 6-311++G(d,p) unless Specified

method	dimer	ΔE[a]	D_e(BSSE)[b]	D_0(BSSE)[c]	D_T[d]	R	A
BLYP	**D1**	3.12	2.88	2.47	1.55	2.285	175.4
BPW91	**D1**	2.66	2.38	2.01	1.08	2.331	175.5
B3LYP	**D1**	3.72	3.46	3.04	1.54	2.234	175.4
B3PW91	**D1**	3.29	3.01	2.60	1.11	2.263	175.3
PW91LYP	**D1**	4.82	4.41	3.93	2.50	2.265	161.0
PW91PW91	**D1**	4.26	3.82	3.34	1.91	2.246	165.5
MP2/6-31G*	**D1**	5.74	3.69	3.12	1.73	2.371	166.9
MP2/6-31+G**	**D1**	5.77	3.89	3.32		2.375	166.7
MP2/6-311G**	**D1**	5.16	3.35	2.78		2.418	168.2
MP2	**D1**	5.37	3.58	3.01		2.417	166.6
B3LYP	**WD**	5.83	5.03	2.70	2.67	1.933	175.6
B3PW91	**WD**	5.28	4.46	2.15	2.13	1.933	175.0
PW91LYP	**WD**	7.37	6.44	4.13	4.10	1.903	173.8
PW91PW91	**WD**	6.79	5.85	3.51	3.52	1.893	174.7
MP2	**WD**	6.08	4.45	2.07	2.04	1.949	176.9
MP2[g]	**WD**	5.31	4.57			1.944	173.0
exptl D_e	**WD**		5.4 ± 0.7[e]				
			5.4 ± 0.2[f]				
B3LYP	**D2**	3.61	3.36	3.02	1.50	2.692	105.7
B3PW91	**D2**	2.98	2.68	2.40	0.82	2.769	106.8
PW91LYP	**D2**	4.84	4.55	4.16	3.26	2.640	104.9
MP2/6-31G*	**D2**	5.26	3.77	3.29	1.84	2.589	103.8
B3LYP	**D3**	3.98	3.26	2.78	1.37	2.471	123.4
B3PW91	**D3**	3.27	2.63	2.17	0.73	2.415	131.2
PW91LYP	**D3**	5.77	4.96	4.40	3.05	2.472	123.0
MP2/6-31G*	**D3**	7.51	4.15	3.53	2.24	2.508	120.1

[a] Total energy difference $\Delta E = nE$(monomer) − E(n-mer). [b] D_e(BSSE) = ΔE + Δ(BSSE). [c] D_0(BSSE) = ΔE + ΔZPE + Δ(BSSE). [d] D_T = ΔE + thermal effect at 298.15 K + Δ(BSSE). [e] From ref 42. [f] From ref 43. [g] Basis set 6-311++G(3df,3pd).

Although in principle diffuse and polarization functions are necessary for van der Waals and weak H-bond systems, the MP2 results (see Table 1) of the dimer **D1** are surprisingly insensitive to the basis sets. For example, the distances R(O···H) vary between 2.37 (6-31G*) and 2.42 (6-311++G**) Å, and the angles A(C−H···O) lie in the 166.6−168.2° range. The estimated binding energies, D_0(BSSE), using the identical ZPE from the small basis set 6-31G* are 3.0 ± 0.3 kcal/mol. The data from B3LYP, B3PW91, and PW91PW91 roughly fall into this range, whereas comparatively, BLYP and BPW91 underestimate D_0(BSSE) to different extents, and PW91LYP overestimates D_0(BSSE). Because the amount of binding energy of the VC dimer is comparable to that of the water dimer (experimental D_e data, 5.4 ± 0.7;[42] 5.4 ± 0.2 kcal/mol[43]), to discuss the reliability of several density functionals to the carbonate complexes, they are also applied (see Table 1) to the most investigated system, the H_2O dimer (noted as WD, C_s symmetry). From Table 1, the values of D_e(BSSE) from B3LYP, B3PW91, and MP2 methods are consistent within 0.5 kcal/mol, and they are also in excellent agreement within the error bars of the two sets of experimental data. However, PW91LYP gives too high D_e(BSSE) value and that from PW91PW91 appears within the error bars of the first experimental result in Table 1 (5.85 vs 5.4 ± 0.7 kcal/mol).

As in the case of **D1**, the binding energies D_0(BSSE) of **D2** and **D3** from PW91LYP are also much higher than those from B3PW91 and B3LYP as well as MP2 methods. Additionally, the order generated by PW91LYP for D_0(BSSE) of the three VC dimers **D1**, **D2** and **D3** is 3.93, 4.16, and 4.40 kcal/mol,

while the order given by B3LYP is 3.04, 3.02, and 2.78 kcal/mol; however, the differences of D_0(BSSE) among dimers are less than 0.5 and 0.3 kcal/mol, respectively, which indicates that the VC dimer potential energy surface is very shallow. The distance of the donor H to the carbonyl O (R) in **D2** is about 0.5 Å longer than that in **D1**, and the C−H···O angle is much smaller than that in **D1** by 60−70°. Although two C−H···O interactions are present in **D2**, the closeness of the D_0(BSSE) values between **D1** and **D2** shows that the interaction energy per C−H···O in **D2** is much weaker than that in **D1**; therefore, like in conventional H-bonds, C−H···O also tends to a linear orientation. The H···O bond length (R) in the T-type of VC dimer, **D3**, is longer than that in **D1** and shorter than that in **D2** by 0.15−0.25 Å; the values of A in **D3** are also between within those of **D1** and **D2**. An AIM calculation in **D3** shows that one bond critical point ($\rho = 0.007$ au) exists between the ethereal oxygen of the H-donor VC molecule and the carbonyl carbon of the H-acceptor VC molecule, and consequently, besides the bond critical point of H···O, a five-membered ring ($\rho = 0.006$ au at the ring critical point) appears between the two VC molecules. Probably, they are responsible for the **D3** binding energy that is comparable to **D1** and **D2**, although only one C−H···O interaction is present instead of two as in **D2** and the interaction is not as strong as that in **D1**.

EC Dimer. The ground state of EC monomer is the nonplanar structure with C_2 symmetry.[44] Two minima (**D4**, **D5**) have been found for the self-associations of EC by intermolecular C−H···O interactions. As shown in Chart 1, **D4** possesses a core empty pseudosandwich structure in which two strong C−H···O interactions ($R \approx 2.45$ and 2.55 Å, respectively, at B3LYP/6-311++G(d,p) level) and one quite weak C−H···O interaction ($R \approx 2.90$ Å) exist. To favor the most stable complex, C−H···O rather deviates from a linear orientation. A is approximately 140° for the C−H···O with the shortest H···O distance, while the other angles are much smaller (115° and 119°, respectively). As for the binding energies summarized in Table 2, a trend similar to that discussed in relation to Table 1 for the several density functionals has also been observed for EC dimer, i.e., exchange functional PW91 and correlation functional LYP result in higher values than their alternatives, B3 and PW91. Consequently, PW91LYP brings about the highest binding energy (D_0(BSSE) ≈ 7.4 kcal/mol), B3PW91 the lowest (D_0(BSSE) ≈ 3.9 kcal/mol), while B3LYP and PW91PW91 methods give moderate values (D_0(BSSE) ≈ 5.1 and 6.1 kcal/mol, respectively). Summing up their performance with respect to VC, EC, and water systems, it is thus probably safe to conclude that B3LYP and PW91PW91 are more proper methods than B3PW91 and PW91LYP methods for the complexes with moderate binding energy (e.g., $D_e \approx 3.0$ kcal/mol per interaction).

To compare the strength of a single C−H···O interaction in VC and EC, another structure of EC dimer is optimized with the single constraint of keeping a linear C−H···O ($R \approx 2.37$ Å). Its binding energy is even higher than half of that of **D4** (D_0(BSSE), 2.9 vs 5.1 kcal/mol), which again shows that the C−H···O interaction has a strong linear tendency. The "head-to-end" structure corresponding to **D2** of VC dimer has also been found for EC dimer (**D5**). The values of R for the two C−H···O interactions in **D5** are about 0.3 Å longer than those of the two short such interactions in **D4** (2.76 vs 2.47 and 2.53 Å at B3LYP/6-311++G** level), and the angles A are considerably small (96.8°). Accordingly, the binding energy is much lower than that of **D4** (D_0(BSSE), 3.68 vs 5.08 kcal/mol at B3LYP level).

TABLE 2: Energy Differences Including Relevant Corrections, ΔE, D_e(BSSE), D_0(BSSE), and D_T (kcal/mol), the Distances between H and Carbonyl O, R (Å), and the Angle of C−H···O, A (deg), for Ethylene Carbonate (EC) Dimers (D4, D5), Propylene Carbonate (PC) Dimer (D6), Dimethyl Carbonate (DMC) Dimer (D7), and the Heteromolecular Dimers of EC and VC (D8, D9), of PC and VC (D10, D11), of EC and PC (D12), of DMC with EC (D13) and PC (D14)

method	dimer	ΔE	D_e(BSSE)	D_0(BSSE)	D_T	R	A
B3LYP	**D4**	6.85	5.93	5.08	4.16	2.466	140.1
						2.950	114.3
						2.534	119.4
B3PW91	**D4**	5.65	4.62	3.90	2.57	2.51	141.6
						2.98	115.0
						2.57	119.9
PW91LYP	**D4**	9.28	8.34	7.44	6.22	2.410	141.4
						2.918	114.5
						2.509	119.1
PW91PW91	**D4**	8.00	6.92	6.11	4.84	2.427	141.7
						2.836	117.4
						2.535	116.4
B3LYP	**D5**	4.47	4.11	3.68	2.16	2.764	96.8
						2.761	96.8
B3LYP	**D6**	6.34	5.38	4.69	3.32	2.466	139.1
						2.578	118.2
						2.835	120.1
B3LYP	**D7**	2.44	2.09	1.66	0.23	2.479	149.5
						2.479	149.2
B3LYP	**D8**	4.32	4.00	3.50	2.04	2.209	174.5
	D9	5.25	4.42	3.80	2.45	2.582	120.4
						2.950	149.9
B3LYP	**D10**	4.49	4.13	3.66	2.20	2.220	176.0
	D11	5.17	4.38	3.87	2.46	2.513	122.7
						3.059	154.6
B3LYP	**D12**	6.73	5.81	5.08	3.75	2.465	139.7
						2.562	118.9
						2.891	118.5
B3LYP	**D13**	4.11	3.41	2.79	1.44	2.501	119.6
						2.523	159.6
B3LYP	**D14**	3.53	2.84	2.31	0.92	2.588	117.4
						2.541	163.7

PC Dimer. The PC dimer geometry (**D6**) looks rather similar to that of EC dimer (**D4**), in which each monomer acts a proton donor as well as a proton acceptor. As shown in Table 2, the distances of H···O for the two relatively strong C−H···O interactions are 2.466 and 2.578 Å respectively, while that for the weak interaction is 2.835 Å, which closely agree with those of **D4** (2.466, 2.534, and 2.950 Å). The C−H···O angles are also very close to those in **D4**. Because of the presence of the electron-donor methyl group, the interaction through C−H···O in PC is slightly weaker than that in EC. This is reflected by the smaller binding energy at the four correction levels, as shown in Table 2 (6.34, 5.38, 4.69, and 3.32 kcal/mol vs 6.85, 5.93, 5.08, and 4.16 kcal/mol); these values correspond to 0.2−0.3 kcal/mol lower per C−H···O interaction. The lower binding energy is also qualitatively consistent with the charges of the complexed H atoms (+0.05 e in EC vs +0.02 e in PC). The binding energy difference per C−H···O interaction between EC and PC associates ($D_T \approx 4.16$ vs 3.32 kcal/mol) should be a main factor leading to the different states at which EC and PC are found at room temperature.

DMC Dimer. The ground state of the monomer DMC is found to have C_{2v} symmetry. The dimer (**D7**) shown in Chart 1 has two nearly identical C−H···O interactions, and they constitute a 10-membered ring confirmed by the AIM calculation (electron density at ring critical point, 0.002 au). The bond distance R

and the angle *A* are 2.479 Å and 149.5°, respectively. The binding energy of the DMC dimer is about two times lower than those of EC and PC (D_0(BSSE), 1.66 vs 5.08 and 4.69 kcal/mol with B3LYP method) and nearly one time lower than that of VC (D_0(BSSE), 1.66 vs 3.04 kcal/mol). Compared with the cyclic carbonate cases such as VC, EC, and PC, the inclusion of temperature effect (298.2 K) especially decreases the binding energy of the linear carbonate dimer.

EC···VC, PC···VC Dimers. Two kinds of cross-association structures of VC with EC and PC have been located, which could have evolved from the planar geometry of **D1** and the T-typed geometry of **D3**, respectively. VC acts as a proton donor in the heteromolecular dimer **D8**. As in **D1**, the C−H···O interaction in **D8** approaches to a linear alignment ($A \approx 176.2°$), and *R* is also quite close to that in **D1** (2.210 vs 2.234 Å), but it has 0.6 kcal/mol higher binding energy than **D1**, indicating that EC is a stronger proton acceptor than VC. Coupled with the fact that the constrained EC dimer holding a C−H···O linear alignment has about 0.2 kcal/mol less binding energy than the VC dimer **D1**, it could be concluded that EC is a weaker proton donor, which is also consistent with the charge carried by the protons (about +0.05 e in EC, about +0.17 e in VC). A short ($R \approx 2.582$ Å, $A \approx 120.4°$) and a relatively long ($R \approx 2.950$ Å, $A \approx 149.9°$) C−H···O interaction are present in the other heteromolecular dimer of EC···VC (**D9**), where VC acts as a proton donor for the former interaction and EC plays the same role for the latter one. The binding energy of **D9** is only 0.4 kcal/mol higher than that of **D8**. PC···VC complexes behave extremely similar to those of EC···VC with respect to structures and binding energies. For example, *R* agrees within 0.01 Å between **D8** and **D10**, and D_0(BSSE) only differs by 0.16 kcal/mol.

EC···PC Dimer. The cross-association structure is rather similar to that of EC dimer and PC dimer themselves, i.e., two short ($R \approx 2.47-2.58$ Å) C−H···O interactions and one long ($R \approx 2.84-2.95$ Å) C−H···O interaction exist in **D12** (see Chart 2). The binding energy D_0(BSSE) is nearly the same as that of the EC dimer **D4** and only 0.4 kcal/mol higher than that of the PC dimer **D6** (5.08 vs 5.08 and 4.69 kcal/mol).

EC···DMC, PC···DMC Dimers. From the Chart 2, the optimized structures for the cross-associations of DMC with EC and PC (**D13** and **D14**, respectively) have two C−H···O interactions. The characteristics of the C−H···O interactions in which DMC acts as a C−H donor are similar to those in the DMC dimer, i.e., the angles *A* tending to be linear (159.6° and 163.7°). Although these cross-associated complexes are more stable than the DMC dimer itself (D_0(BSSE), 2.75 and 2.31 vs 1.66 kcal/mol), they are much less stable than the EC dimer and the PC dimer, as well as the cross-associated complexes of EC and PC. The results together with the aforementioned of EC···PC could provide an explanation to the experimental fact that a pure EC solution presents intermolecular association that remains unaltered in the presence of PC but it is disrupted by a linear carbonate such as DMC.[2] Most probably PC/DMC could also associate with the EC molecule in their mixtures; however, cyclic carbonate molecules as a whole still behave as associates instead of as free molecules in the mixture of EC and PC because of their close binding energies, while the weak binding between EC and DMC could increase the fluidity of their mixture. On the basis of this point, both PC and VC are not as good as the linear carbonate DMC for use as EC cosolvents.

VC and EC Trimers. Energetic and selected geometrical data are shown in Table 3. Three different local minima have been found for VC trimers. Two of them (**T1** and **T2**, C_s and C_{2v} symmetry, respectively, as shown in Chart 2) hold planar geometry, while the two C−H acceptor molecules are perpendicular to the C−H donor molecule in another trimer (**T3**, C_{2v} symmetry). **T1**, **T2**, and **T3** could be taken as evolutions from **D1**, **D2**, and **D3** dimers, respectively, by complexing one more VC molecule. In line with the conventional H-bond systems, such as H_2O and methanol,[41,45] the global minimum **T1** also corresponds to a cyclic structure in which each VC acts as a C−H donor as well as an acceptor (see Chart 2). The three C−H···O interactions are almost identical, which is reflected by their *R* (2.2350, 2.2301, and 2.2383 Å), and *A* values (164.6°, 164.1°, and 164.7°) and other characteristics such as bond lengths and vibrational frequencies of C−H, electron density, and Laplacian of the electron density at the H···O bond critical point. In the case of the open trimer **T2**, only the central VC molecule behaves as C−H···O donor and acceptor simultaneously, while the two end molecules behave either as donor or as acceptor. The four weak C−H···O interactions are slightly different. **T2** lies 2.99 kcal/mol above the global minimum. Another open structure trimer, **T3**, with the middle VC molecule as a double C−H donor, is predicted to be 4.65 kcal/mol less stable than the global minimum **T1**. As expected, this complex is symmetric, with two identical C−H···O interactions ($R \approx 2.506$ Å, $A \approx 123.5°$ at B3LYP/6-311++G** level). On the

CHART 2: Optimized Geometries (B3LYP/6-311++G(d,p)) of Carbonate Dimers and VC and EC Trimers

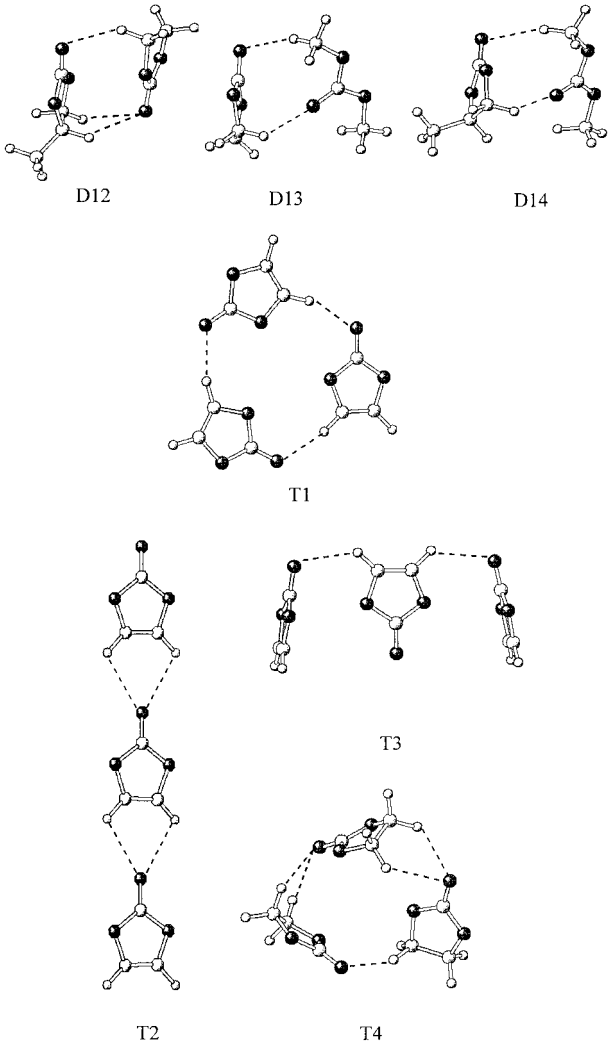

TABLE 3: Energy Differences Including Relevant Corrections, ΔE, D_e(BSSE), D_0(BSSE), and D_T (kcal/mol), the Distances between H and Carbonyl O, R (Å), and the Angles of C−H···O, A (deg), of VC Trimers (T1, T2, and T3) and EC Trimer (T4)

method	trimer	ΔE	D_e(BSSE)	D_0(BSSE)	D_T	R	A
B3PW91	**T1**	10.74	9.46	8.18	5.55	2.263	164.5
						2.261	164.9
						2.257	164.8
PW91LYP	**T1**	15.70	14.56	13.42	10.60	2.178	165.1
						2.183	164.9
						2.175	165.2
B3LYP	**T1**	12.16	11.06	9.70	7.06	2.238	164.7
						2.235	164.6
						2.230	164.1
B3LYP	**T2**	8.03	7.43	6.71	3.68	2.6624	105.4
						2.6635	105.1
B3PW91	**T3**	6.09	4.75	3.88	0.98	2.442	131.6
B3LYP	**T3**	7.57	6.04	5.05	2.23	2.506	123.5
PW91LYP	**T4**	18.49	16.37	14.63	12.11	2.395	140.6
						2.403	139.7
						2.412	131.8
B3LYP	**T4**	13.84	12.06	10.59	7.86	2.339	153.3
						2.823	120.1
						2.418	132.1
						2.540	131.1
						2.634	127.0

other hand, the binding energy per C−H···O interaction is about 0.3 kcal/mol weaker than that in the corresponding dimer **D3** (D_0(BSSE)/per interaction of 2.5 vs 2.8 kcal/mol), which is consistent with the reduction of the positive charge carried by the donor H upon formation of the first C−H···O in **T3**. It is worth mentioning that a similar structure for the water trimer was also found to be a minimum (structure **1a**),[45] in which the per HB (O−H···O) is 0.5 kcal/mol (HF/6-311++G(2d,d2p)) less stable than that in the global minimum, and it is also 0.3 kcal/mol lower than that of the dimer.

Only the most probable global minimum has been optimized for the EC trimer. As was previously found for VC trimers, it is also a cyclic structure, but the three monomers are in quite different locations (**T4**, see Chart 2). It looks like two monomers arrange similarly to the EC dimer (**D4**) keeping one end apart from each other so that the third monomer is inserted. Consistently, five different C−H···O interactions (R = 2.339, 2.823, 2.418, 2.540, 2.634 Å) are present. The total binding energy is about 0.9 kcal/mol higher than that of the VC trimer **T1** (10.59 vs 9.70 kcal/mol).

The strength of the C−H···O interactions in cyclic carbonate molecules is comparable to that of O−H···O in water. For example, the cases **D1** and the constrained EC dimer, in which one interaction is well-defined, have slightly higher binding energy than the water dimer (D_0(BSSE) = 3.0, 2.9, and 2.7 kcal/mol). The presented C−H···O interaction of cyclic carbonates is even stronger than that in formamide dimer, where the binding energy of C−H···O was estimated to be 2.3 kcal/mol[46] (without ZPE, at MP2/aug-cc-pVDZ level; 3.6 for **D1** with MP2 and comparable basis set 6-311++G(d,p)). As in the water and formamide systems, therefore, considerable associations also exist among carbonate molecules in the form of dimers, trimers, etc., which would remarkably affect their physical properties.

B. Characteristics of C−H···O Interactions Using AIM. The AIM theory[15] allows one to identify and characterize bonding interactions between atoms through an analysis of the charge density, ρ. In a series of studies, Koch and Popelier proposed a set of criteria (composed of local properties of the electron density, ρ, Laplacian of the electron density, $\nabla^2\rho$, at the bond critical point along the interaction path, and integrated properties of donor H) that are indicative of H-bond.[47,48] Bond critical points between the hydrogen atom and the carbonyl oxygen atom are found in all C−H···O interactions, except for those cases in which R is beyond 2.7 Å such as the one in dimer **D4** ($R \approx 2.95$ Å) and both in **D5** ($R \approx 2.76$ Å), etc. According to the previous studies, the electron density, ρ, at the bond critical point associated with normal hydrogen bonding varies typically in the range of 0.002−0.034 au,[47,48] e.g., 0.025 and 0.027 au for O−H···O H-bonds at B3LYP/6-311+G(d,p) in water and methanol dimer, respectively,[41] which are sensibly lower than those of covalent bonds. ρ at the bond critical point of H···O shown in the second column of Table 4 varies from 0.0060 au in **D2** to 0.0138 au in **D10**, fitting well within the range of values for normal H-bond interactions. Although the binding energy per C−H···O interaction in **D1** is even higher than that of O−H···O in the water dimer (D_0(BSSE), 3.04 vs 2.70 kcal/mol at B3LYP/6-311++G(d,p) level) and very comparable to that in methanol dimer (D_0(BSSE), both 3.5 kcal/mol),[41] the magnitude of ρ in **D1** is only half of that in water and methanol dimers (0.013 vs 0.025 au). The values of ρ in **D1**, **T1**, and two cases in **T4** are very similar to that of the intramolecular C−H···O in aromatic *N*-sulfinylaniline, i.e., phenyl−N=S=O (0.013 au)[17] as well as the C−H···π interaction of $HCCl_3$ with benzene (0.011 au).[16] As it was found for water systems (O−H···O)[45] and C−H···π interactions,[16] except for **D7** of the linear carbonate DMC, a good linear correlation (see Figure 1, correlation coefficient r = 0.95) exists between the binding energies per C−H···O interaction and the averaged electron density ρ at the corresponding bond critical points (the number of interactions for the dimers of EC and PC are 2, it is 4 for the trimer of EC, **T4**). Therefore, the electron density at the bond critical points bears a direct relationship with the strength of C−H···O within these cyclic complexes, and accordingly the values of ρ may be a good index to directly discuss the relative stability of such interactions.

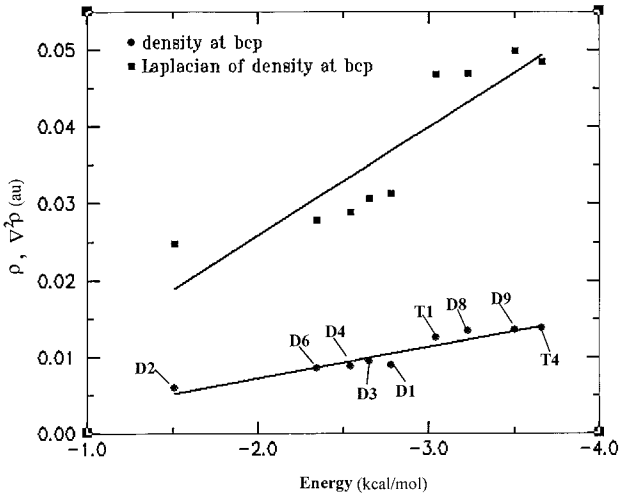

Figure 1. Electron density (au, ●) and its Laplacian (au, ■) at the bond critical point (bcp) against the BSSE- and ZPE-corrected interaction energy (kcal/mol) per C−H···O interaction for some carbonate dimers and trimers.

It has been established that the value of $\nabla^2\rho$ at the bond critical point in conventional H-bonds, and more generally for closed-shell interactions such as ionic bonds and van der Waals complexes, is positive. All of the complexes shown in Table 4 (the third column) meet this requirement, and the values of $\nabla^2\rho$ at the bond critical point of H···O, which vary between 0.025 and 0.050 au, are similar to the range of values for typical

TABLE 4: Electron Densities (ρ) and Laplacian of the Electron Densities ($\nabla^2\rho$) at the Bond Critical Points of H···O, at the H-Bond Donor C−H, and at the C═O Linkage of the Acceptor Moiety and Charges of the H Atom Involved[a]

compound	ρ(H···O)	$\nabla^2\rho$(H···O)	q(H)	ρ(C−H)	$\nabla^2\rho$(C−H)	ρ(C═O)	$\nabla^2\rho$(C═O)
VC			0.1692	0.2897	−1.039	0.4391	−0.1567
D1	0.0125	0.0469	0.2101	0.2904	−1.054	0.4342	−0.1923
D2	0.0060	0.0248	0.1988	0.2910	−1.050	0.4348	−0.1869
D3	0.0089	0.0313	0.2146	0.2909	−1.055	0.4340	−0.2080
T1	0.0134	0.0470	0.2314	0.2900	−1.057	0.4306	−0.2367
EC			0.0480	0.2842	−0.9813	0.4381	−0.1875
			0.0468	0.2860	−0.9975		
D4	0.0091	0.0288	0.0905	0.2881	−1.011	0.4322	−0.2454
	0.0085	0.0290	0.0774	0.2887	−1.019	0.4316	−0.2538
T4	0.0084	0.0271	0.0775	0.2893	−1.024	0.4304	−0.2640
	0.0073	0.0233	0.0693	0.2889	−1.014	0.4304	−0.2640
	0.0102	0.0345	0.1285	0.2896	−1.027	0.4297	−0.2691
	0.0119	0.0378	0.1133	0.2893	−1.021	0.4304	−0.2630
PC			0.0196	0.2855	−0.9940	0.4374	−0.1941
D6	0.0091	0.0289	0.0548	0.2883	−1.012	0.4314	−0.2516
	0.0079	0.0268	0.0616	0.2881	−1.014	0.4308	−0.2657
	0.0051	0.0175	−0.0045	0.2879	−1.005	0.4308	−0.2657
DMC			0.0289	0.2834	−0.977	0.4212	−0.2883
D7	0.0083	0.0276	0.0459	0.2864	−1.001	0.4181	−0.3046
VC/EC			0.1692	0.2897	−1.039	0.4381	−0.1875
D8	0.0135	0.0499	0.2010	0.2901	−1.054	0.4328	−0.2286
VC/PC			0.1692	0.2897	−1.039	0.4374	−0.1941
D10	0.0138	0.0485	0.1764	0.2899	−1.053	0.4319	−0.2419
H_2O			0.3904	0.3663	−2.491	0.3663	−2.491
WD	0.0246	0.0929	0.4509	0.3555	−2.474	0.3640	−2.511

[a] All values in au obtained at the B3LYP/6-311++G(d,p) level.

H-bonded interactions, which can vary from 0.014 to 0.139 au.[47] Again, $\nabla^2\rho$ of **D1**, **T1**, **D8**, and **D10** compare well with those of the intramolecular C−H···O in aromatic *N*-sulfinylaniline (0.048 au)[17] and the C−H···π interaction between $HCCl_3$ and benzene;[16] however, they are significantly lower than those for water and methanol (∼0.09).[41] A slightly rough linear correlation (see Figure 1, correlation coefficient $r = 0.9$ excluding the datum of **D7**) also exists.

Another important feature for the formation of H-bond is the loss of the donor hydrogen atom charge because of its descreening upon complex formation. By comparison with that in the isolated monomer, the data in the fourth column in Table 4 clearly show that the net charge of the donor hydrogen atom increases to a different extent. The magnitude of the effect varies from 0.01 to 0.08 e. Two exceptions are observed in which the charge decreases for the hydrogen atoms of a longer C−H···O ($R \approx 2.835$ Å in **D6**, $R \approx 2.823$ Å in **T4**). Therefore, although a bond critical point exists between the corresponding hydrogen and oxygen atoms (as shown in Table 4, **D6**) and the values of ρ as well as $\nabla^2\rho$ lie within the range of a normal hydrogen bond, the C−H···O interaction could not be classified as a hydrogen bond. The correlation between the average charge increment and the binding energy per interaction is not as good as that for ρ and $\nabla^2\rho$.

Other necessary conditions of H-bond for the donor hydrogen atom are also checked to further confirm hydrogen bonding of C−H···O, i.e., energetic destabilization and decrease of dipolar polarization of the donor H atom. The former can be demonstrated by the higher total energy of the donor H upon complexation. As shown in Table 5, the energy increments for the donor H in **D1** and **T1** agree well with the destabilization observed in water dimer. Although quite low, the quantities (0.0077 and 0.0142 au) for the donor H in **D2** and **D7** also lie in the range for normal H-bonds.[47] Table 5 also shows that the complexation results in the reduction of first moments of the donor H between 0.015 (**D7**) and 0.044 (**D2**), which also meets the necessary condition for H-bond that a dipolar polarization decreases for the complexed hydrogen atom.

TABLE 5: Integrated Atomic Energy and the First Moment of the H Atom in the Isolated Momomer (H_{iso}) and in the Complex (H_{com}) and the Change (Δ) Arising from Association[a,b]

	H_{iso}	H_{com}	Δ
D1	−0.5758	−0.5541	0.0217
	0.1225	0.0897	−0.0328
T1	−0.5708	−0.5433	0.0275
	0.1293	0.0977	−0.0316
D2	−0.5585	−0.5508	0.0077
	0.1345	0.0906	−0.0439
D7	−0.6092	−0.5950	0.0142
	0.1428	0.1274	−0.0154
WD	−0.3913	−0.3691	0.0222
	0.1510	0.1081	−0.0429

[a] The first row for each complex refers to energy and the second to first moment. [b] All values in atomic units.

The preceding results show that C−H···O interactions clearly exist in these dimers and trimers. These interactions, either the proton donor linked with an unsaturated carbon of VC or with a saturated one of EC/PC/DMC, exhibit similar topological features of the electron density at bond critical points of H···O, and close variations among the integrated properties of the donor H, including positive electron density and positive Laplacian of the electron density within the range for H-bond and suffering from a loss of electron density, an energetic destabilization, and a reduction in dipolar polarization. Moreover, the criteria for H-bond are fulfilled with respect to local properties of electron density at the bond critical point along the interaction path and integrated properties of the donor H. The C−H···O interactions ($R > 2.7$ Å excluded) investigated here may be classified as H-bond.

C. Binding Analysis Using ELF. One of the major advantages of the ELF technique is that it can directly reveal the local character of binding between two adjacent atoms. Even though a clear onset, if any, has not been well-developed, in general a low-valued saddle point exists in the ELF values between two atoms for a van der Waals dominant interaction (e.g., about 0.05 for the homonuclear dimers of group 12 elements[34]), while

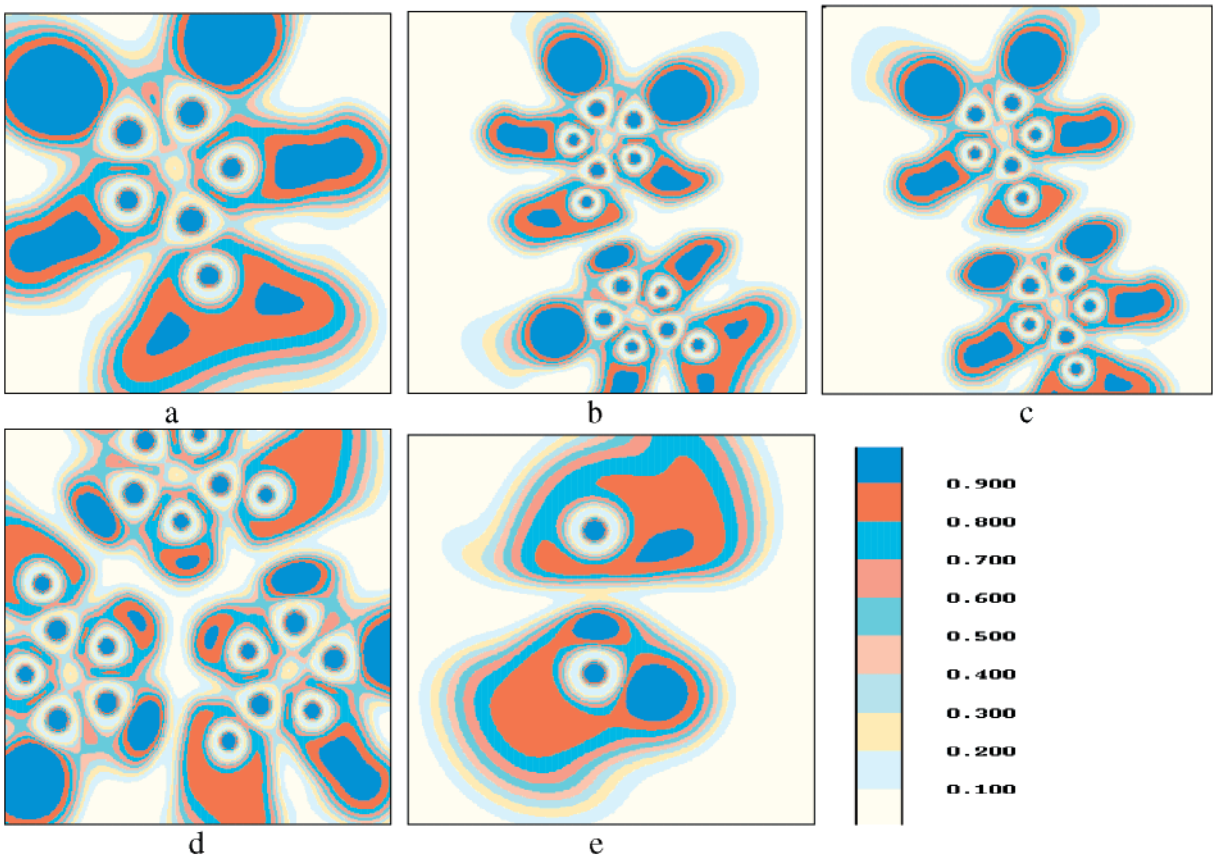

Figure 2. Two-dimensional plots of ELF. The ELF values are encoded by colors. Shown are (a) VC molecule, (b) VC dimer, **D1**, (c) VC dimer, **D2**, (d) VC trimer, **T1**, and (e) water dimer.

a high-valued maximum occurs for typical covalent interactions. As to the H-bond and the weak bond with nonnegligible covalent character (e.g., ELF = 0.29 for Yb_2[35]), the ELF value should lie in between. Two-dimensional ELF plots are investigated only for the VC monomer (Figure 2a), VC dimers (Figure 2b,c for **D1** and **D2**, respectively), and VC trimer (Figure 2d, **T1**). For comparison, a 2D ELF picture is also made for the water dimer in the section through H-donor water and the oxygen atom of the other molecule (Figure 2e). Figure 2a exhibits the presence of the two lone pairs of electrons on the carbonyl O atom in the form of two tear drops, with ELF = 0.90. As shown in Figure 2b, it is evident that the topological structure is only preserved in the C−H donor VC moiety and is distorted in the acceptor moiety in which one high ELF (0.9) domain remains unchanged, but for the other one, ELF is reduced upon the formation of the C−H···O H-bond. The lone pairs of electrons in the system therefore play an important role in establishing the H-bond. Moreover, a saddle point of ELF = 0.20 is observed between the carbonyl O atom and the donor hydrogen atom. The ELF value is nearly the same as that of water dimer (Figure 2e). In the case of **D2** (see Figure 2c), a high banana-shaped ELF region shows variations in the lone electron pairs of the carbonyl O atom upon formation of H-bonds. The lower ELF value (0.14) of a saddle point is in good agreement with its longer H-bond distance compared to that in **D1**. As it was previously found for clusters of group 12,[34] the ELF values at the saddle points also dominantly depend on the atomic distances. In the case of **T1** (Figure 2d), the ELF values at the three saddle points of the H-bond are identical (ELF = 0.21), and they are also rather close to that in **D1** because of the closer atomic distance (2.23 vs 2.24 Å). Consistent with the AIM calculation, among the three inner ethereal oxygen atoms, the island with low ELF value (ELF = 0.08) also indicates that a quite weak interaction exists there.

TABLE 6: Length (*L*, Å) and Harmonic Vibration Frequencies (ν, cm^{-1}) of the C−H Bond for the Monomer (M) and of the C−H···O Interactions of Dimers (D1, D2, and D3) and Trimers (T1, T2, and T3) of VC[a]

			ν^a		$\Delta\nu$	
	L	ΔL	ν_s	ν_{as}	$\Delta\nu_s$	$\Delta\nu_{as}$
M	1.0748		3315 (a1)	3290 (b2)		
D1	1.0772	0.0024	3308	3271	−7	−19
D2	1.0738	−0.0010	3330	3306	15	16
D3	1.0756	0.0008	3312	3288	−3	−2
T1	1.0785	0.0037	3309	3255	−6	−35
	1.0785	0.0037	3309	3254	−6	−36
	1.0787	0.0039	3308	3252	−7	−38
T2	1.0737	−0.0011	3331	3307	16	17
	1.0736	−0.0012	3333	3309	18	19
T3	1.0754	0.0006	3313	3289	−2	−1

[a] Values obtained at the B3LYP/6-311++G(d,p) level.

D. Bond Lengths and Vibrational Frequencies for C−H of Donor Molecules. The C−H harmonic frequencies of the two vibrational modes for the isolated VC molecule are 3315 (a_1) and 3290 cm^{-1} (b_2) at B3LYP/6-311++G(d,p). They are quite sensitive to the exchange functionals, while they change only a little with correlation functionals, e.g., 3323 and 3298 cm^{-1} at B3PW91, 3235 and 3212 cm^{-1} at PW91LYP, 3252 and 3228 cm^{-1} at PW91PW91. The C−H bond lengths and harmonic vibrational frequencies of VC dimer and VC trimers have been summarized in Table 6. It can be observed that in the dimer **D1** the H-bond donor C−H is stretched by 0.0024 Å, while the free C−H and those of the H-bond acceptor remain practically unchanged (therefore not shown in Table 6).

TABLE 7: Length (*L*, Å) and Harmonic Vibrational Frequencies (ν, cm^{-1}) of the C−H Bond for the Monomer (M) and of the H-Bond of EC Dimer (D4) and Trimer (T4)[a]

L(M)	*L*(**D4**)	Δ*L*(**D4**)	*L*(**T4**)	Δ*L*(**T4**)	ν(M)	ν(**D4**)	Δν(**D4**)	ν(**T4**)	Δν(**T4**)
1.0888	1.0873[b]	−0.0015	1.0871[b]	−0.0017	3135 (1b)	3154	+19	3158	+23
1.0929			1.0885[c]	−0.0044	3123 (1a)	3137	+14	3146	+23
					3058 (2b)	3078	+20	3094	+36
					3054 (2a)	3060	+6	3066	+12
	1.0906[c]	−0.0023	1.0869[b]	−0.0019		3144	+9	3159	+24
						3127	+4	3143	+20
						3081	+23	3087	+29
						3061	+7	3060	+6
			1.0899[c]	−0.0030				3151	+16
								3130	+7
								3088	+30
								3062	+8

[a] Values obtained at the B3LYP/6-311++G(d,p) level. [b] Associated with the shorter C−H bond of EC monomer. [c] Associated with the longer bond of EC monomer.

Consequently, in the dimer **D1**, the C−H vibrational frequencies of the donor show red shifts of 7 and 19 cm^{-1}, which corresponds to a_1 and b_2 modes in the isolated monomer (termed as symmetric, ν_s, and antisymmetric, ν_{as}, hereafter for *n*-mers). The coupling between the two C−H stretching vibrations is not totally removed even for the H-bond donor. The stretch of the donor C−H and the red shift of its vibrational frequency are approximately five and six times less than that of methanol dimer (0.015 Å and 148 cm^{-1} at B3LYP/6-311++G(d,p)), respectively.[41] In the case of **D3**, there exists a minor C−H stretch (0.0008 Å) and a negligible C−H frequency change (less than 5 cm^{-1}). The C−H stretch and red shift are also observed for the other cases in which VC acts as H-bond donor, such as the heteromolecular dimers **D8** (ΔL = 0.0031 Å, $\Delta\nu_{as}$ = −27 cm^{-1}), **D9** (ΔL = 0.0010 Å), **D10** (ΔL = 0.0036 Å, $\Delta\nu_{as}$ = −39 cm^{-1}), and **D11** (ΔL = 0.0011 Å).

In contrast to the cases of **D1**, **D3**, and the heteromolecular dimers, **D2** exhibits a C−H contraction (0.0010 Å) and accordingly a blue shift of vibrational frequencies (15 and 16 cm^{-1} for ν_s and ν_{as}, respectively), i.e., anti-hydrogen-bond behavior. The results show that the C−H···O interaction of donor H linked with sp^2 hybridization carbon may demonstrate the characteristics of a normal hydrogen bond as well as those of an anti-hydrogen bond, which quite depends on the bond angle of C−H···O. For a nearly linear case such as **D1**, it performs similarly to the cases of C−H donor with sp and sp^2 unsaturated hybridization, such as the interactions of acetylene and HCN with benzene[16] and acetylene and ethylene with H_2O,[14] while for the very bent C−H···O interactions ($A \approx 100°$) it resembles the sp^3 hybridization of C like $F_nH_{3-n}CH$.[11] To get more insights into the variations of the characteristics for C−H···O interactions with its angle, a series of structures between a linear C−H···O alignment and **D2** are partially optimized by holding the C−H···O angle (*A*). The potential energy curve is so shallow that both the forward energy barrier (ΔE) to the formation of a linear structure or **D1** and the backward barrier are less than 0.1 kcal/mol. The relevant parameters of the transition state are *R*(H···O) = 2.2402 Å, *L*(C−H) = 1.0742 Å, *A* = 127.7°, ν_{as} = 3298 cm^{-1}, and ν_s = 3323 cm^{-1}, and it is characterized by its sole imaginary frequency (−19 cm^{-1}). Like in the dimer **D1**, the C−H···O in the structure with linear C−H···O behaves as a normal H-bond (*R* = 2.2400 Å, *L* = 1.0773 Å, ν_{as} = 3271 cm^{-1}, and ν_s = 3307 cm^{-1}). It appears that the C−H···O interactions with *A* less than about 130.0° have the characteristics of an anti-hydrogen bond, such as the cases of *A* = 106° (*L* = 1.0738 Å), *A* = 116° (*L* = 1.0734 Å), and *A* = 126° (1.0743 Å); otherwise they behave as the normal H-bond, e.g., *A* = 136° (*L* = 1.0749 Å), *A* = 146° (*L* = 1.0757 Å), and *A* = 166° (1.0769 Å). The result is somewhat in agreement with the intramolecular C−H···O interaction in aromatic *N*-sulfinylaniline, in which the angle of C−H···O is about 130° at B3LYP/6-311++G(d,p) and the shortened C−H bond (about 0.003 Å) shows a blue shift of 26 cm^{-1}.[17]

With respect to the trimer **T1**, the C−H bond of the donor is further stretched ($\Delta L \approx 0.0037$ Å), which results in about one time higher red shift for ν_{as} but a negligible change for ν_s as compared with those in **D1**. The higher stretching frequency shift could be taken as an evidence of nonnegligible cooperative effects in the VC trimer, **T1**. The cooperative factor ($A_b \approx 2.0$ for **T1**) defined in terms of the relative shift of the C−H stretching frequency shows that cooperativity is considerably important in the three C−H···O H-bonds of the VC trimer. The other associated quantities also confirm this. As illustrated in Table 1 and Table 3, the higher binding energy per C−H···O interaction in **T1** than in **D1** (3.23 vs 3.04 kcal/mol at B3LYP/6-311++G**) implies that there is a net energy gain of about 0.6 kcal/mol in the formation of **T1**. The greater lengthening (ΔL) of the C−H bonds shown in Table 6 for **T1** than for the dimer (**D1**) is another clear indication of the significant cooperative effect in **T1**. In the cases of **T2** and **T3**, Table 6 shows that only minor quantitative changes take place for length and frequency shifts of the donor C−H, and qualitatively the C−H···O interactions keep the same characteristics as **D2** and **D3**, respectively.

Four fundamental modes, 1*a*, 2*a*, 1*b*, and 2*b*, are associated with the stretches of C−H in EC. The bond lengths for free C−H in the monomer, *L*(M), and only those for the C−H involved in H-bond in the dimer and trimer, *L*(D) and *L*(T), together with their corresponding vibrational frequencies are listed in Table 7. Opposite effects to VC complexes are observed upon the formation of a H-bond. The C−H bonds are considerably contracted, and consistently a blue shift takes place on the C−H vibrational frequencies (e.g., as shown in Table 7, ΔL = −0.0015 Å, the largest $\Delta\nu$ = +23 cm^{-1} for the EC dimer; the averaged ΔL = −0.0028 Å, the largest $\Delta\nu$ = +36 cm^{-1} for EC trimer). The trend is maintained for the other dimers involved here and is extended to the trimers as well, e.g., ΔL = −0.0017 Å for the DMC dimer, ΔL = −0.0015 Å for the PC dimer, and ΔL = −0.0021 Å for the heteromolecular dimer of EC and DMC (**D13**), etc. This shows that an anti-hydrogen-bond character in terms of the C−H bond contraction and blue shift would occur in the cases for which a donor H is linked to a saturated carbon, i.e., sp^3 hybridization. The present result for EC dimers and trimer agrees well with the C−H···O interactions of methane and fluorinated methane with the proton

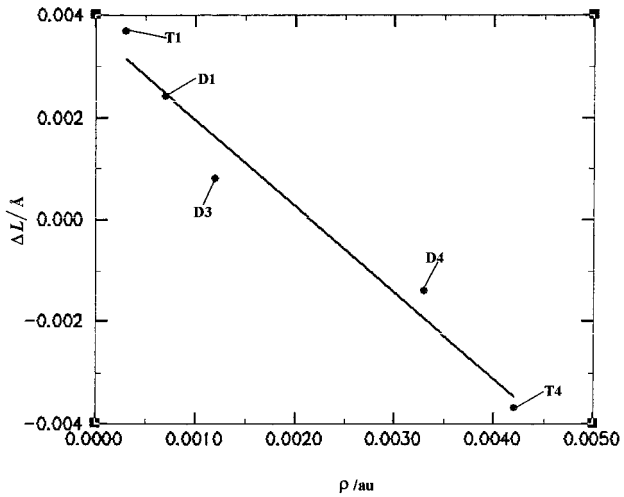

Figure 3. Representation of the shift in bond length (Å) with the change in electron density (au) at the C−H bond critical points for VC and EC complexes.

acceptors, such as H_2O, CH_3OH, and H_2CO.[8,11] It is also noted that Table 7 shows clear indications for H-bond cooperative effects in EC trimer, e.g., greater shortening of its C−H bonds and high associated blue shifts of their stretching frequencies.

E. Remarks on C−H Bonds of Donor Molecules. The topological properties of electron densities at the hydrogen bond (H···O) critical points discussed in the preceding sections show no relevant difference for the two sorts of carbonate complexes, even though the results in Tables 6 and 7 indicate that there is a fundamental division between the complexes exhibiting features of conventional H-bond or anti-H-bond behavior in terms of C−H bond length and its stretching frequency. To get more insights into the unusual hydrogen bonding (C−H···O) behavior in EC dimers and trimers, the topological characteristics of the electron density at the bond critical points for the proton donor C−H and proton acceptor C═O bonds are also summarized in Table 4 together with those of the water dimer. As to the proton acceptors, the C═O in carbonate complexes and the O−H in the water dimer, these two different interactions exhibit similar variations in ρ and $\nabla^2\rho$, i.e., reduction of the former and more negative values of the latter. Regarding the proton donors (C−H bond), the results show that the electron density is considerably enhanced by 0.0020−0.0050 au for the H-bond with antinormal character and that it is only slightly enhanced by less than 0.0010 au for those VC serving as proton donors, whereas the electron density for the O−H in water dimer is 0.0108 au lower than that in the isolated monomer. As it was stated by Cubero et al. for the C−H···π systems,[16] it is worth noting that such a difference between the two sorts of C−H···O actually relates to the corresponding variations in bond length. Specifically a good correlation exists, as shown in Figure 3 (correlation coefficient $r = 0.98$), between the change in electron density at the bond critical point of the C−H bond and the corresponding variations in bond length, ΔL. Although $\nabla^2\rho$ exhibits an opposite variation for the O−H (less negative) and C−H (more negative) bonds upon the formation of the corresponding H-bond, they behave similarly for the two sorts of C−H···O interactions, i.e., $\nabla^2\rho$ becomes more negative by a change of a similar magnitude.

The motivation of establishing the origin of the different behaviors of C−H···O interactions in EC and VC complexes leads us to perform a simple analysis of another important molecular property, the dipole moment. First of all, the local dipole moments of the H-bond donor groups (C−H) have opposite orientations, e.g., the charge distributions of the C−H groups in VC and EC monomers are $q_C = -0.0403$ e, $q_H = +0.1692$ e (at B3LYP/6-311G** level) and $q_C = +0.1584$ e, $q_H = +0.0468$ e, respectively. These trends are also true for other typical molecules, such as H_2O ($q_O = -0.7808$ e, $q_H = +0.3905$ e), acetylene ($q_C = -0.2309$ e, $q_H = +0.2309$ e), and CH_3F ($q_C = +0.2022$ e, $q_H = +0.0290$ e). The hydrogen bond (O−H···O) in H_2O dimer and that (C−H···O) in acetylene with oxygen-containing proton acceptors exhibit similar behavior to the C−H···O in VC dimer, as does the C−H···O in CH_3F with proton acceptors to that in EC dimer. It is worth noticing that the local dipole moment of the C−H donor in EC dimer changes its orientation ($q_C = +0.0616$ e, $q_H = +0.0900$ e) perhaps to adjust itself to the same orientation as the acceptor group C═O. However, in the VC dimer it keeps the same orientation as that in the monomer. These differences may be related to the C−H bond contraction (stretch) in the EC dimer (VC dimer). On the other hand, as in the case of H_2O and acetylene, we find that the moment of the monomer molecule is increased by the stretch of the C−H bond in the VC monomer, whereas it is lowered when the C−H bond stretches in EC. The variation data of the dipole moment are summarized in Table 8. The C−H bond contraction in EC dimer would increase to some extent the total stabilization energy of the complex through enhancing the electrostatic attraction. Therefore, as claimed by Gu et al.[11,49] for the C−H···O and O−H···O systems, the opposite effect of a C−H bond stretch on the monomer dipole moment is at least one of the possible reasons for the observed C−H contraction in the EC dimer and a stretch in the VC dimer.

TABLE 8: The Variations of Molecular Dipole Moments ($\Delta D \times 10^3$, D) with One of the C−H Bonds ($\Delta L \times 10^2$, Å) around the Equilibrium Geometries for VC and EC

ΔL	1.5	1.0	0.5	0	−0.5	−1.0	−1.5
ΔD (EC)	−6	−4	−2	0	3	5	7
ΔD (VC)	2	2	1	0	0	−1	−2

Conclusions

In this paper, we have reported a comprehensive study of associations for VC, EC, PC, and DMC in gas phase. Our results are summarized as follows: (1) The exchange functional PW91 generally overestimates the binding energy (about 3.0 kcal/mol per interaction) for the C−H···O interactions present in alkyl carbonate molecules, although it is an appropriate functional for the much weaker systems, such as N−H···π H-bond (D_e(BSSE) $\approx$ 2.0 kcal/mol) in ammonia−benzene systems.[23−26] We conclude that B3LYP and PW91PW91 are more proper methods than B3PW91 and PW91LYP methods for the H-bond systems with energies of about 3.0 kcal/mol per interaction. (2) The C−H···O H-bond between cyclic carbonate molecules is much stronger than that between the linear carbonate molecules, and the total binding energies of the global minimal homomolecular dimers decrease in the order of EC > PC > VC > DMC (D_0(BSSE) of 5.08 > 4.69 > 3.04 > 1.66 kcal/mol). On the basis of the similarities among the heteromolecular dimer of EC/PC, and the EC and PC respective homomolecular dimers in terms of both energetic and geometric properties, it can be concluded that PC may not destroy the associated structure of EC in their mixture, whereas the differences between the heteromolecular dimer of EC/DMC and the homomolecular dimers of EC and DMC may lead to the conclusion that EC would be less-associated in the mixture of EC with DMC. (3) On the basis of the AIM calculation, the characteristics of C−H···O interactions are identified with a set of criteria for conventional H-bonds. For the two cases in

which the proton donor is linked with an unsaturated carbon of VC and with a saturated one such as EC/PC/DMC, although the C−H···O interactions exhibit opposite variations in C−H bond length and its vibrational frequency, they have similar topological features of the electron density at bond critical points of H···O and close variations are observed among the integrated properties of the donor H, including positive electron density and positive Laplacian of electron density within the range for a conventional H-bond, characterized by a loss of electron density, an energetic destabilization, and a reduction in dipolar polarization. Moreover, the criteria for H-bond are fulfilled with respect to the local properties of the electron density at the bond critical point along the interaction path and integrated properties of the H donor. Therefore, the C−H···O interactions (R > 2.7 Å excluded) investigated here could be classified as H-bond. (4) Consistent with the AIM analysis, ELF nicely demonstrates the existence of clear C−H···O interactions for VC dimers and trimer, which shows that the ELF technique is also useful for the characterization of C−H···O systems. (5) A good correlation between the change in electron density at the bond critical point of the C−H bond and its corresponding variations in bond length ΔL indicates that the electron density at the bond critical point of the C−H bond does not suffice to distinguish between the two kinds of C−H···O interactions either; however, the opposite effects of a C−H bond stretch upon the monomer dipole moment perhaps can be made responsible for the observations of a C−H contraction in the EC dimer and a stretch in the VC dimer.

Acknowledgment. This work was partially supported by NSF (Career Award Grant CTS-9876065 to P.B.B.), by Mitsubishi Chemical Corporation, and by DOE Cooperative Agreement DE-FC02-91ER75666. We acknowledge supercomputer resources provided by the National Computational Science Alliance under Grants CHE000040 N, CTS000016 N, CTS00007 N (Y.W., P.B.B.) and by the National Energy Research Scientific Computing Center, NERSC.

References and Notes

(1) Aurbach, D.; Levi, M. D.; Levi, E.; Schechter, A. *J. Phys. Chem. B* **1997**, *101*, 2195.
(2) Klassen, B.; Aroca, R.; Nazri, M.; Nazri, G. A. *J. Phys. Chem. B* **1998**, *102*, 4795.
(3) Li, T.; Balbuena, P. B. *J. Electrochem. Soc.* **1999**, *146*, 3613.
(4) Jehoulet, C.; Biensan, P.; Bodet, J. M.; Broussely, M.; Tessier-Lescourret, C. *Batteries for Portable Applications and Electric Vehicles*; The Electrochemical Society Proceedings Series; The Electrochemical Society: Pennington, NJ, 1997.
(5) Fujii, A.; Fujimaki, E.; Ebata, T.; Mikami, N. *J. Am. Chem. Soc.* **1998**, *120*, 13256.
(6) Jedlovszky, P.; Turi, L. *J. Phys. Chem. B* **1997**, *101*, 5429.
(7) Houk, K. N.; Menzer, S.; Newton, S. P.; Raymo, F. M.; Stoddart, J. F.; Williams, D. J. *J. Am. Chem. Soc.* **1999**, *121*, 1479.
(8) Scheiner, S.; Gu, Y.; Kar, T. *J. Mol. Struct.: THEOCHEM* **2000**, *500*, 441.
(9) Scheiner, S. *Hydrogen Bonding. A Theoretical Perspective*; Oxford University Press: New York, 1997.
(10) Hobza, P.; Havlas, Z. *Chem. Phys. Lett.* **1999**, *303*, 447−452.
(11) Gu, Y.; Kar, T.; Scheiner, S. *J. Am. Chem. Soc.* **1999**, *121*, 9411.
(12) Hobza, P.; Havlas, Z. *Chem. Rev.* **2000**, *100*, 4253.
(13) Desiraju, G. R. *Acc. Chem. Res.* **1996**, *29*, 441.
(14) Hartmann, M.; Wetmore, S. D.; Radom, L. *J. Phys. Chem. A* **2001**, *105*, 4470.
(15) Bader, R. F. W. *Atoms in molecules, a quantum theory*; Clarendon Press: Oxford, 1990.
(16) Cubero, E.; Orozco, M.; Hobza, P.; Luque, F. J. *J. Phys. Chem. A* **1999**, *103*, 6394.
(17) Muchall, H. M. *J. Phys. Chem. A* **2001**, *105*, 632−636.
(18) Becke, A. D.; Edgecombe, K. E. *J. Chem. Phys.* **1990**, *92*, 5397−5403.
(19) Savin, A.; Becke, A. D.; Flad, J.; Nesper, R.; Preuss, H.; Schnering, H. G. v. *Angew. Chem., Int. Ed. Engl.* **1991**, *30*, 409.
(20) Parr, R. G.; Yang, W. *Density Functional Theory of Atoms and Molecules*; Oxford University Press: Oxford, 1989.
(21) Perez-Jorda, J. M.; Becke, A. D. *Chem. Phys. Lett.* **1995**, *233*, 134.
(22) Hobza, P.; Sponer, J.; Reschel, T. *J. Comput. Chem.* **1995**, *16*, 1315.
(23) Zhang, Y.; Pan, W.; Yang, W. *J. Chem. Phys.* **1997**, *107*, 7921.
(24) Patton, D. C.; Pederson, M. R. *Phys. Rev. A* **1997**, *56*, R2495.
(25) Wesolowski, T. A.; Parisel, O.; Ellinger, Y.; Weber, J. *J. Chem. Phys. A* **1997**, *101*, 7818.
(26) Enkvist, C.; Zhang, Y.; Yang, W. *Int. J. Quantum Chem.* **2000**, *79*, 325.
(27) Becke, A. D. *Phys. Rev. A* **1988**, *38*, 3098.
(28) Perdew, J. P. Unified theory of exchange and correlation beyond the local density approximation. In *Electronic Structure of Solids*; Ziesche, P., Eschrig, H., Eds.; Akademie Verlag: Berlin, 1991.
(29) Becke, A. D. *J. Chem. Phys.* **1993**, *98*, 5648.
(30) Lee, C.; Yang, W.; Parr, R. G. *Phys. Rev. B* **1988**, *37*, 785.
(31) Boys, S. F.; Bernardi, F. *Mol. Phys.* **1970**, *19*, 553.
(32) Huyskens, P. L. *J. Am. Chem. Soc.* **1977**, *99*, 2578.
(33) Savin, A.; Nesper, R.; Wengert, S.; Fässler, T. F. *Angew. Chem., Int. Ed. Engl.* **1997**, *36*, 1808−1832.
(34) Flad, H.-J.; Schautz, F.; Wang, Y.; Dolg, M.; Savin, A. *Eur. Phys. J. D* **1999**, *6*, 243−254.
(35) Wang, Y.; Schautz, F.; Flad, H.-J.; Dolg, M. *J. Phys. Chem. A* **1999**, *103*, 5091−5098.
(36) Wang, Y.; Flad, H.-J.; Dolg, M. *J. Phys. Chem. A* **2000**, *104*, 5558−5567.
(37) Trout, B. L.; Parrinello, M. *J. Phys. Chem. B* **1999**, *103*, 7340−7345.
(38) Frisch, M. J.; Trucks, G. W.; Schlegel, H. B.; Scuseria, G. E.; Robb, M. A.; Cheeseman, J. R.; Zakrzewski, V. G.; Montgomery, J. A., Jr.; Stratmann, R. E.; Burant, J. C.; Dapprich, S.; Millam, J. M.; Daniels, A. D.; Kudin, K. N.; Strain, M. C.; Farkas, O.; Tomasi, J.; Barone, V.; Cossi, M.; Cammi, R.; Mennucci, B.; Pomelli, C.; Adamo, C.; Clifford, S.; Ochterski, J.; Petersson, G. A.; Ayala, P. Y.; Cui, Q.; Morokuma, K.; Malick, D. K.; Rabuck, A. D.; Raghavachari, K.; Foresman, J. B.; Cioslowski, J.; Ortiz, J. V.; Stefanov, B. B.; Liu, G.; Liashenko, A.; Piskorz, P.; Komaromi, I.; Gomperts, R.; Martin, R. L.; Fox, D. J.; Keith, T.; Al-Laham, M. A.; Peng, C. Y.; Nanayakkara, A.; Gonzalez, C.; Challacombe, M.; Gill, P. M. W.; Johnson, B. G.; Chen, W.; Wong, M. W.; Andres, J. L.; Head-Gordon, M.; Replogle, E. S.; Pople, J. A. *Gaussian 98*, revision A.9; Gaussian, Inc.: Pittsburgh, PA, 1998.
(39) Schautz, F. Program for the Evaluation of ELF. Max-Planck Institute: Dresden, Germany, 2001.
(40) Molpro is a package of ab initio programs written by Werner, H.-J. and Knowles, P. J. with contributions from: Almloef, J.; Amos, R. D.; Deegan, M. J. O.; Elbert, S. T.; Hampel, C.; Meryer, W.; Nicklass, A.; Peterson, K.; Pitzer, R. M.; Stone, A. J.; Talyor, P. R.; Werner, H.-J.; Knowles, P. J. *Theor. Chim. Acta* **1990**, *78*, 175. Hampel, C.; Peterson, K.; Werner, H.-J. *Chem. Phys. Lett.* **1992**, *190*, 1.
(41) MÓ, O.; Yáñez, M. *J. Chem. Phys.* **1997**, *107*, 3592.
(42) Curtiss, L. A.; Frurip, D. J.; Blander, M. *J. Chem. Phys.* **1979**, *71*, 2703.
(43) Reimers, J.; Watts, R.; Klein, M. *Chem. Phys.* **1982**, *64*, 95.
(44) Wang, Y.; Nakamura, S.; Ve, M.; Balbuena, P. B. *J. Am. Chem. Soc.*, in press.
(45) MÓ, O.; Yáñez, M.; Elguero, J. *J. Chem. Phys.* **1992**, *97*, 6628.
(46) Vargas, R.; Garza, J.; Friesner, R. A.; Stern, H.; Hay, B. P.; Dixon, D. A. *J. Phys. Chem. A* **2001**, *105*, 4963.
(47) Koch, U.; Popelier, P. L. A. *J. Phys. Chem.* **1995**, *99*, 9747.
(48) Popelier, P. L. A. *J. Phys. Chem. A* **1998**, *102*, 1873.
(49) Hobza, P.; Spirko, V.; Havlas, Z.; Buchhold, K.; Reimann, B.; Barth, H.-D.; Brutschy, B. *Chem. Phys. Lett* **1999**, *299*, 180−186.